EUROPEAN FUSION DEVELOPMENT AGREEMENT

EFDA–JET–CP(04)02/27

M. Becoulet, G. Huysmans, P. Thomas, E. Joffrin, F. Rimini, P. Monier-Garbet, A. Grosman, P. Ghendrih, V.Parail, P. Lomas, G. Matthews, H. Wilson, M. Gryaznevich, G. Counsell, A.Loarte, G. Saibene, R. Sartori, A.Leonard, P. Snyder, T. Evans, P. Gohil, R. Moyer, Y. Kamada, N. Oyama, T.Hatae, K. Kamiya, A.Degeling, Y. Martin, J. Lister, J. Rapp, C. Perez, P. Lang, A. Chankin, T.Eich, A. Sips, J. Stober, L. Horton, A. Kallenbach, W. Suttrop, S. Saarelma, S. Cowley, J. Lönnroth, M. Shimada, A. Polevoi, G. Federici and JET EFDA Contributors

Edge Localized Modes Control: Experiment and Theory

Edge Localized Modes Control: Experiment and Theory

M. Becoulet[1], G. Huysmans[1], P. Thomas[1], E. Joffrin[1], F. Rimini[1], P. Monier-Garbet[1], A. Grosman[1], P. Ghendrih[1], V.Parail[2], P. Lomas[2], G. Matthews[2], H. Wilson[2], M. Gryaznevich[2], G. Counsell[2], A.Loarte[3], G. Saibene[3], R. Sartori[3], A.Leonard[4], P. Snyder[4], T. Evans[4], P. Gohil[4], R. Moyer[5], Y. Kamada[6], N. Oyama[6], T.Hatae[6], K. Kamiya[6], A.Degeling[7], Y. Martin[7], J. Lister[7], J. Rapp[8], C. Perez[8], P. Lang[9], A. Chankin[9], T.Eich[9], A. Sips[9], J. Stober[9], L. Horton[9], A. Kallenbach[9], W. Suttrop[9], S. Saarelma[10], S. Cowley[11], J. Lönnroth[12], M. Shimada[13], A. Polevoi[13], G. Federici[14]
and JET EFDA Contributors[*]

[1]Association Euratom-CEA, CEA Cadarache, F-13108 St. Paul-lez-Durance, France.
[2]Euratom/UKAEA Association, Fusion Culham Science Centre, Abingdon, OX14 3EA, UK.
[3]EFDA Close Support Unit, 2 Boltzmannstrasse, Garching, DE.
[4]General Atomics, 3550 General Atomics Court,P.O.Box 85608 San Diego, CA, U.S.A.
[5]University of California, San Diego, La Jolla CA 92093,U.S.A.
[6]Japan Atomic Energy Research Institute (JAERI), 801-1 Mukoyama, Naka-machi, Naka-gun 311-0193, Japan
[7]Centre de Recherches en Physique des Plasmas, Association Euratom-Confédération Suisse, Ecole Polytechnique Fédérale de Lausanne,CH-1015 Lausanne, Switzeland.
[8]Institut für Plasmaphysik, Forschungszentrum Julich, Germany.
[9]Association Euratom-IPP, MPI fur Plasmaphysik, 2 Boltzmannstrasse, Garching, D-85748, Germany
[10]Helsinki University of Technology, Euratom-TEKES Association, FIN-02015 HUT, Finland.
[11]Department of Physics,Imperial College,Prince Consort Road,London,SW7 2BZ,UK.
[12]Euratom-Tekes, Helsinki University of Technology, P.O. Box 2200, 02015 HUT,Finland.
[13]ITER International Team,, Mukouyama, Naka-machi, Naka-gun, Ibaraki-ken 311-0193, Japan
[14]ITER JWS Garching Co-center, Boltzmannstraße2, 85748 Garching, Germany
See annex of J. Pamela et al, "Overview of Recent JET Results and Future Perspectives", Fusion Energy 2002 (Proc. 19th IAEAFusion Energy Conference, Lyon (2002).

Preprint of Paper to be submitted for publication in Proceedings of the
16th PSI Conference,
(Portland Maine, USA 24-28 May 2004)

ABSTRACT

The paper reviews recent theoretical and experimental results focussing on the identification of the key factors controlling ELM energy and particle losses both in natural ELMs and in the presence of external controlling mechanisms. Present experiment and theory pointed out the benefit of the high plasma shaping, high q_{95} and high pedestal density in reducing the ELM affected area and conductive energy losses in Type I ELMs. Small benign ELMs regimes in present machines (EDA, HRS, Type II, Grassy, QH, Type III in impurity seeded discharges at high δ) and their relevance for ITER are reviewed briefly. Recent studies of active control of ELMs using stochastic boundaries, small pellets and edge current generation are presented.

1.INTRODUCTION

Edge Localised Modes (ELM) represent Magneto Hydro Dynamics (MHD) instabilities in the pedestal region typical for H-mode scenarios [65], [6], [62], [3]. They provide burst-like energy and particle transport through the External Transport Barrier (ETB) on a fast MHD time scale (few τ_{Alfven}) in a quasiperiodic way followed by a phase of the pedestal pressure profile rebuilding. The strong link between the maximum achievable plasma confinement and ELM regimes is well established in present tokamaks [54], [19], [62], [58] In particular, the most studied Type I ELMs, occurring when applied power is above L/H transition threshold $P_{thL/H}$ by factor of 1.5-2 [58], correspond to the high confinement H-mode scenario foreseen for ITER with I_p=15MA, q_{95}=3, τ_{burn}~400s, $Q=P_{fusion}/P_{loss}$=10, β_N~1.8, H_{98y2}=1, n/n_{GR}~0.8 [17]. At the same time energy losses in Type I ELMs in ITER can be problematic for the divertor target plates leading to the melting, erosion, and evaporation of the materials [13]. According to the present estimations for carbon (CFC) and tungsten (W) divertor plates, the acceptable lifetime for target (>10^6 Type I ELMs, ~3000 ITER pulses) can be achieved if the energy loss from the pedestal per ELM do not exceed 5MJ-14MJ. This represents about 5-15% of the pedestal energy estimated as W_{ped}^{ITER}~110MJ [13]. According to the present experimental data [11] it was assumed that about 65% of the pedestal energy loss in ELM reaches the target. Also the energy deposition time to the divertor was varied from 0.1ms to 1ms for low and upper limit respectively Due to the large uncertainties in the previous assumptions and to the statistical properties of Type I
ELMs themselves [37] the extrapolation for ITER still remains an open question, but is still too marginal to be optimistic, motivating the present study of control of Type I ELMs.

Type III ELM regimes are usually observed if input power is between $1.<P_{in}/P_{thL/H}<1.5$-2 [58] and are characterized by high frequency and acceptably small energy losses per ELM. But at the same time the poor confinement of such regimes is not sufficient for a standard H-mode scenario in ITER [17]. Recent investigation of high triangularity impurity seeded (N_2) discharges in JET suggest the possibility of an H-mode scenario with Type III ELMs for ITER with the reference plasma current increased to 17MA [51]. However, impurity injection remains questionable issue because of their accumulation in the plasma.

Another scenario proposed for ITER is based on the Internal Transport Barrier (ITB) creation in the reversed magnetic shear (RS) configuration (Ip=9MA,q_{95}=5, τ_{burn}>3000s, Q=5, β_N~2.8,H_{98y2}=1.6) [17]. Apart from the significant difficulties to sustain the RS profile because of the limited possibilities of non-inductive current drive in ITER, also Type I ELMs will represent a problem for such scenario. In particular, Type I ELMs cause an erosion of the ITB [18] and are hardly avoidablable especially in the high triangularity (δ~0.5) ITER-like configuration [2, 3], [59]. The Hybrid (or Advanced) scenario without ITB, but still pre-formed q-profile q_o>~1 to avoid saw-teeth, hasdemonstrated higher performance than the standard H-mode: H_{98y2}=1.3, n/n_{GR}~0.88, β_N~3.5, β_p~1.8. It was first observed in AUG [Sips2002] and more recently in JET [34]. The Hybrid scenario proposed for ITER (I_p=12MA, q_{95}=5, τ_{burn}>1000s, Q=5.5, β_N~2.3,H_{98y2}=1) faces the same restrictions for Type I ELM regime as H-mode.

The possible combination of high confinement (close to Type I ELMs regimes) Hmodes and small benign edge MHD activity instead of large energy bursts was demonstrated in many tokamaks in specific plasma conditions (discussed later in the paper). However, Grassy ELMs [23], Type II regimes [61], [55], EDA [20], HRS [25, 26], QH mode [4] have been obtained in a narrow operational windows that not match ITER parameters [3]. Some of these small ELM regimes can be combined with improved core confinement [15]. In particular ITBs with Grassy ELMs [24] and High Recycling Steady (HRS) Hmode [25, 26] were obtained, Quiescent Double Barrier (QDB) [18] with QH mode, and high β_p Advanced (or Hybrid) scenarios with Type II ELMs [Sips2002] and Grassy ELMs [24], were demonstrated but still their extrapolation for ITER is an open question.

Summarising the present day experiments, the natural regimes with acceptable ELMs and high confinement are difficult to achieved in ITER. The experimental multi-machine comparative studies and the improved theoretical understanding of the key factors determining ELM size are urgently required for extrapolation for ITER. This situation has motivated recent experimental and theoretical development of active ELMs control using externally imposed control mechanisms. In particular stochastic boundaries [14], [42], [12], small pellets [29], edge parallel current generation by vertical plasma displacements in an inhomogeneous magnetic field [8] and in plasma current ramps experiments [58], [14], [3] were tried as ELM control tools.

The paper reviews recent theoretical and experimental results focussing on the identification of the key factors controlling ELM energy and particle losses for natural and externally induced ELMs. The recent results of ideal linear MHD stability analysis, non-linear explosive evolution of ballooning modes and transport modelling with Type I ELMs are presented in Sec.2. In Sec.3 the convective and conductive losses behaviour is discussed with respect to the changes in triangularity, q_{95} factor, density, collisionality. In particular conditions the burst-like transport in Type I ELMs can be replaced by a more continuous (in time) edge MHD activity providing increased transport through ETB. These benign ELMs regimes in present tokamaks and their operational domains are presented briefly. Sec.4. revises presently known techniques of active ELMs control such as edge ergodisation by external coils, pellets and edge current generation using plasma current ramps and vertical oscillations of plasma column. Conclusions and discussion are presented in Sec.5.

2. PROGRESS IN THEORY

The most dangerous for the ITER divertor and hence the most studied Type I ELMs have similar characteristics in all tokamaks. In particular the temperature and density crash first on the Low Field Side (LFS) as seen on many diagnostics suggests the presence of the ballooning like instability [45, 46], [44], [36], [7]. The characteristic time of the pedestal crash (~200-300μs) and the MHD signature observed on the magnetic probes are also similar [37], [3].

The destabilisation of the peeling and ballooning modes driven by the edge parallel current density (mainly by the large bootstrap current fraction) and the edge pressure gradient respectively are considered presently as candidates for Type I ELM triggers [6], [64], [60], [21], [31]. The development of the ideal linear MHD stability codes for ballooning and peeling modes and their confrontation against the experimental data suggest that the main mechanism of Type I ELMs is identified. For example, the maximum achievable pedestal pressure in experimental Type I ELMs regimes correspond to the calculated ideal MHD limit for coupled ballooning–peeling modes [60] (Fig1(a)). The improvement of the pedestal confinement with plasma shaping (triangularity) was demonstrated in many machines [23], [61], [54], [55] and was also explained by MHD stability calculations. The improvement of edge stability is attributed to the increased magnetic shear and the possible access to the second stability regime at high triangularity. [60], [2], [53], [40]. The eigenmode width calculated by the stability codes in most cases corresponds to the experimentally found ELM affected area [Leonard2001], [60], [31], [38]. All these facts gives a confidence for the stability calculations for ITER [60] (see Fig.1(b-c)) The pedestal width scaling for ITER remains the main uncertainty. However with reasonable assumptions for ITER pedestal parameters one can expect the ideal coupled ballooning -peeling mode destabilisation and hence Type I ELMs.

Linear codes are limited in the description of the ELM dynamics. A recently proposed non linear model suggest that ballooning modes can develop explosively giving birth to narrow finger–like structures pushing aside other field lines and spreading the instability over a large plasma region [Cowley2003]. 3D non-linear Braginskii calculations with BOUT-code [Xu2002] also suggest the bursty transport to the SOL due to ballooning modes at least in the early non-linear stage [60]. For the moment this image of Type I ELMs is not developed that far to reproduce ELM cycles.

In 1,5D transport codes pedestal transport during ELMs was traditionally modelled by increasing the perpendicular heat or particle transport coefficients in the ETB region affected by ELM by a large factor when the edge pressure gradient exceeds the critical value ($\alpha>\alpha_{crit}$) for ballooning modes or when the edge current profile becomes unstable ($j>j_{crit}$) [22], [48]. In the next step model for Type I ELM in JETTO [40] the transport coefficients in the ELM affected area are increased proportionally to the sum of the unstable modes amplitudes calculated from the differential equations suggested by linear ideal MHD theory. Each edge magnetic surface is tested against ideal stability criteria for ballooning and peeling modes separately [6], [64]. The mode amplitude grows exponentially when the normalised pressure gradient α exceeds the critical gradient α_{crit} for ballooning modes and $j>j_{crit}$ for peeling modes. The mode amplitude decreases with a given rate

once pressure gradient or current are relaxed below the critical values ($\alpha=\alpha_{crit}$ or $j=<j_{crit}$). This typical decay time for the ideal modes is a parameter in modelling but is chosen according to the observed experimental MHD Type I ELM time (~200μs). This model reproduces well the typical Type I ELM cycles (Fig.2(a)) suggesting initial ballooning mode destabilisation and a fast crash followed by a longer peeling unstable phase since current is reacting with a resistive time delay. This leads too the unrealistic too long ELM crash (few ms) as it was mentioned also in [22]. However edge current can change much more rapidly then the diffusive time scale since it can be lost due to the reconnections with the open field lines. Notice that ELM cycle can be changed by the specific conditions. For example the pure peeling ELMs can be triggered while the plasma current is ramping-up (Fig.2(b)) and pure ballooning ELMs if edge current is reduced in current ramp-down [40].

Similar ideology for a growth rate calculation for ballooning modes is adapted in 2D transport code TELM [3] coupled with ideal MHD code MISHKA [21], with the difference that the non-linear TELM model calculates additional conductive and convective fluxes appearing in MHD phase. These fluxes are generated mainly due to the velocity and radial magnetic perturbations (zero in the stable phase), suggesting the effective "ergodisation" of the perturbed edge magnetic surfaces and convection being the main mechanism of increased transport in ELM. Recent experimental observations of the fines structures in the diveror power deposition in AUG [10] suggest an ergodic-like pattern resulting from a helical perturbation n=8-24 on the LFS. However the energy transport from perturbed closed magnetic surfaces trough the separatrix to the open field lined in the Scrape-Of-Layer (SOL) and a parallel transport to the divertor is very simplified in TELM, still leaving the consistent ELM description and the most important prediction of ELM size for the future.

3. KEY FACTORS LIMITING ENERGY AND PARTICLE LOSSES IN TYPE I ELMS. SMALL ELMS REGIMES

In spite of the fact that the present status of the ELM theory cannot predict the size of the ELMs there are at least a number of theoretical suggestions how to decrease ELM affected pedestal volume. In particular the beneficial effects of high triangularity, high safety factor, high β_p in increasing of edge magnetic shear and decreasing the ELM affected area were largely discussed in the recent literature [60], [31], [53], [48], [2, 3], [39]. On the other hand the improved edge stability at high triangularity usually leads to the higher maximum achievable density in these regimes (n/n_{GR}~0.8-1). The density increase is playing an indirect role in the edge stability first in decreasing characteristic diffusion time and the edge bootstrap current [60], [Becoulet 2001], [48], [40] and second, leading to the increased transport in ETB [48], [3]. The comparison of the experimentally identified ELM affected area by subtraction of the pedestal density and temperature profiles before and after ELM [Leonard2001] [37], and calculated eigenmodes width are clearly correlated in DIII-D [60], JT-60U [31], AUG [53] and JET [38]. However the ELM size is not linked to the eigenmodes width in a simple way since there are many experimental examples when ELMs energy losses varies by

factor of 3 with unchanged ELM affected area [38]. The separation of convective ($\sim\Delta n^{ELM}T$) and conductive($\sim\Delta T^{ELM}n$) energy losses in Type I ELM [32] demonstrated similar dependences on plasma parameters and magnetic configurations in many tokamaks [37, 38], [33], [7]. In particular it was shown that the conductive losses decrease strongly with the pedestal density while the particle convective losses fraction remains almost constant [33], [37]. For example in JET these "minimum" only particle convective ELMs were observed in mixed regimes with Type II ELMs at rather high density $\sim n_{GR}$ (ν^*>0.6-0.8) .The remaining Type I ELM's size is decreased by a factor of ~2 as compared to the same frequency Type I ELMs in similar un-fuelled discharges [2], [36]. The other important factor decreasing conductive losses is high edge safety factor. Small ($\Delta W_{ELM}/ W_{ped}$ ~<5%) convective ELMs were demonstrated in JET at high ITER-like triangularity (δ~0.5) and high q_{95}>4.5 even at low collisionality: ν^*~0.06 (see Fig.3 taken from [38]). The theoretical explanation of the different dependence of convective and conductive losses on plasma parameters is still missing. However the rather low collisionality (ν^*=0.07-0.16) high confinement (usually like with Type I ELMs : H_{98y2}~1) Grassy ELMs regimes observed at high δ~0.55 and high q_{95}>6 in JT- 60U [23] could be the manifestation of the same trend in Type I ELM behaviour in strong edge shear configurations. Stability calculations for AUG benign Type II ELMs regimes also demonstrated a strong decrease in ELM affected area at high triangularity, high q_{95}>4.5 [53]. As compared to JT-60U rather high density (~0.8n_{GR}) and Double Null (DN) configuration are also required. The specific feature of the benign ELMs regimes is the increased level of density and magnetic fluctuations characterized by a broadband frequency spectrum (<30kHz) [61], [2], [55]. This suggests the existence of a mechanism increasing the transport through the ETB [55]. For example the high toroidal numbers n ideal ballooning modes [39], or resistive Washboard modes are proposed as a Type II ELMs mechanism [49].

H-modes without Type I ELMs such as the EDA regime observed in Alcator-C-Mod [20], the High Recycling Steady (HRS) regime in JFT-2M [25, 26, 27] can be observed at high pedestal collisionality ν^*>1.-5. Such high collisionality regimes are hardly achievable in present machines [35] and even less in ITER (ν^*>0.05). A common feature of H-modes without ELMs as edge MHD activity observed in EDA and HRS in the form of Quasi Coherent (QC) mode was associated with a resistive ballooning mode according to stability calculations [43].

Low collisionality ν^*~0.05 Quiescent H-mode(QH) without ELMs was first observed in DIII-D [4], [18] and reproduced in AUG [63], JT-60U [56, 47]. Plasma shaping is not very important in this regime, but there are a number of other specific conditions. In particular, a high upper clearance configuration, low density (0.1-0.4 n_{GR} depending on the machine) and the, most important, counter (opposite to the plasma current direction, which is not foreseen for ITER) neutral beam injection are required for QH regime. Resulting poor particle confinement, high Z_{eff} ~3.3-5 are the most common features for these regimes. The presence of the of the Edge Harmonics Oscillations(EHO) with the main toroidal number n=1, then n=2,3,4 (possibly external kink or tearing modes) is also the main feature of these regime. All H-modes with benign small ELMs discussed above support

the idea that in certain conditions the pedestal transport can be selforganized in a form of continuous MHD and turbulent activity sufficiently small not to loose high confinement H-mode but at the same time resulting in avoidance of the large Type I ELMs crashes.

4.EXTERNAL MECHANISMS OF TYPE I ELMS CONTROL

According to the present knowledge, non of discussed above benign ELM regimes is directly applicable for ITER, but their physics suggested new ideas of the external control mechanisms mainly based on the pedestal pressure and current profiles control.

4.1 STOCHASTIC BOUNDARY

It is well known that a small resonant (qres=m/n) magnetic perturbation from external coils can create a stochastic layer in the plasma, where the perpendicular diffusion can be effectively increased by the diffusive-like behaviour of the magnetic lines [52], [57]. The transport in a stochastic magnetic field was largely studied mostly in circular machines [16], [41], [1]. The first application of ergodic fields in H-modes in COMPASS-D [14] demonstrated the transition from ELM-free to ELMy regime (possibly Type III) when the radial magnetic perturbation was applied. Edge density and temperature decrease was observed, confirming the interpretation of increased transport in the stochastic layer. On the contrary, almost complete suppression of Type I ELM in high triangularity Hmodes was demonstrated in DIII-D at constant confinement [12] (see Fig.4). The external magnetic perturbation from the I-coils (I_{coil}=4.4kA) (Fig4(i)) mainly with toroidal number n=3 was used. The effect was demonstrated in the range of q_{95}=3.5-4 confirming its resonant nature. Electron pressure profile is unchanged as compared to Type I ELMs (Fig.4(g)), indicating probably only marginally increased transport in ETB, but the recycling level for C^{IV} is increased with the ergodic field (Fig.4(h)). The increased level of edge MHD was observed while the I-coil perturbation was applied (Fig4(f)) similar to [14]. The observed decrease of the toroidal plasma rotation (Fig.4(e)) which was expected in the presence of the static perturbation applied at the edge, did not perturb the the H-mode in present experiment, but in principle can have a destabilising effect. For example the lower threshold for the error fields penetration and hence lock modes and disruptions are observed at lower toroidal rotation [5]. The possibility to reach the ELM suppression without plasma braking (for example applying the oscillating perturbation) is one of the goals for future experiments [12].

4.2 PELLETS

The control of the ELM frequency and size by pellets is intensively studied on AUG [29]. The fact that pellets usually trigger an ELM was known from the plasma fuelling experiments [28]. The aim of the ELM control by pellets is to trigger ELMs with given size, but to avoid over-fuelling of main plasma and decreasing the global confinement. It was demonstrated [29] that the injection of small (~1.4mm^3, ~6.10^{19}D-atom, V~560m/s, High Field Side) pellets in AUG can trigger ELMs with the pellet injection frequency f_{pellet} without over-fuelling if $f_{intrinsic} < f_{pellet} <$~20Hz, where $f_{intrinsic}$

is natural Type I ELM frequency without pellets (Fig.5). The electron pressure profiles (however slightly lower gradients were observed for pellets), magnetic signature, heat loads on the divertor plates of pellet trigered ELMs are very close to the intrinsic ELMs with similar frequency [29]. This suggests probably the same nature of the destabilized MHD modes. However, since the ELM is triggered after ~200μs after pellet enters in plasma and only ~20% of pellet mass is ablated up to this time the pellet still represents an inhomogeneous 3D plasmoid leading to a large anisotropy in the edge pressure and hence the obvious limitations of the applicability of the ideal MHD theory for such ELMs. Also pedestal collisionality is usually increased by pellets, since the pedestal density is higher and temperature lower for the pellet triggered ELMs as compared to intrinsic ones [29]. This fact was in particular the main motivation for modelling of pellet controlled ELMs for ITER [50].The numerical estimations demonstrated the possibility of pellet triggered ELMs in Q=10 H-mode scenario with f_{ELM}~4Hz at $\Delta W_{ELM}/W_{ped}$<5% since the pedestal collisionality is increased by such pellets up to ν^*~1.

4.3 EDGE CURRENT

Another control tool suggested by the ideal MHD stability theory is edge current density [21], [64], [60], [40]. The possibilities to change edge current are limited in present machines since the reliable current drive techniques are not known at the plasma edge. However the edge current can be changed in current ramp experiments since the resistive time($\sim T_e^{-3/2}$) at the edge is much lower then in the plasma centre, leading to the local increase and decrease of the parallel current density in ramp-up and down phase respectively. The ELM cycle (Fig.2) can be modified, changing the ELM regime. Edge current can play a stabilising role giving the access to the second stability for ballooning modes, but further increase of the edge current density can destabilise low npeeling modes. When edge plasma is peeling unstable the change in the ELM regime to the Type III ELMs [58] or dithering L-mode [3] with lower confinement were observed. In current ramp-down experiments [58], [3] on the contrary the transition from Type III to Type I ELMs were observed and hence the improvement in the pedestal stability. Current ramp experiments confirmed the main trends given by the ideal MHD stability theory. However the possibility of ramping current (and in particular dI_p/dt) usually is limited by technical limits specific for the machines. Depending also on the resistive time, the plasma response can be rather slow (~0.5s in JET [3] [58]).

More rapid change of edge current density is possible using the technique of vertical displacements of the plasma column first done in COMPASS-D [14] and more recently in TCV with vertical control coils [8]. The rapid change in time of the magnetic flux due to such displacements produces surface voltage and hence the edge current. It was demonstrated that ELM frequency locks to the frequency of these oscillations (Fig.6). At present these ELMs are interpreted as a manifestation of peeling instability occurring periodically due to the periodic changes in the edge current density. The amplitude for triggered ELMs (estimated from D_α signal) follows to the same experimental scaling almost linear in f_{ELM} as natural ELMs [8]. First optimistic estimations of such a technique

for ELM control in ITER using external poloidal coils were done [8] but further experimental investigations on larger tokamaks is required.

CONCLUSIONS AND DISCUSSION

The destabilisation of ballooning and peeling modes in the region of steep edge gradients in H-mode is largely supported by experimental data as a triggering mechanism at least for Type I ELM. Present linear ideal MHD stability codes predict maximum pedestal pressure, observed in experiments. The beneficial effect of high triangularity is also explained in the frame of ideal MHD theory. The ELM affected area measured in experiment approximately correspond to the calculated eigenmode width in many tokamaks. Recently developed pedestal transport models with Type I ELMs based on ideal MHD, but including pressure profile relaxation, permit to model the complete ELM cycle from the fast crash on MHD time scale (200μs) to the pedestal rebuilding phase on a diffusive time scale (typically few ms). Early non-linear phases of ELM crash models based on Braginskii equations and explosive model for ballooning modes suggest narrow toroidally localized structures developing after a linear phase leading to a particle bursts into the SOL.

The present status of the modelling does not permit self-consistent calculations of energy and particle losses in ELMs. Nevertheless both theory and experiment suggest the benefit of high plasma shaping (triangularity), high q_{95} and high pedestal density on the reduction of the size of Type I ELMs. In particular the most important conductive part ($\sim\Delta T^{ELM}n$) of energy lost during the ELM decreases strongly not only with density (collisionality) as it was identified previously but also at high q_{95}, leading to the small ($\Delta W_{ELM}/W_{ped}<5\%$) mainly convective ELMs, which were observed in JET.

Small benign ELMs regimes (EDA, HRS, Type II, Grassy, QH) were demonstrated in present machines in very specific conditions regarding magnetic configuration and pedestal parameters, and are not applicable directly to ITER. However it is worth to stress that the most common feature for many of small ELM high confinement H-modes is the increased MHD or turbulence activity replacing large busty transport in Type I ELMs by a continuous transport mechanism through ETB. If such kind of mechanism can be generated externally in controlled way keeping high confinement regime at the same time it could be the way to complete ELMs suppression.

Active control of Type I ELMs is progressing in present tokamaks. The possibility of almost complete Type I ELMs suppression by edge ergodisation at constant confinement was demonstrated in DIII-D. ELM frequency and size can be controlled by small pellets (AUG) minimising confinement degradation due to the fuelling as compared to the gas injection. The experiments on TCV demonstrated the possibility of locking ELMs frequency on a frequency of rapid vertical plasma oscillations induced by position control coils. This effect is attributed to the induction of the surface voltage and hence the edge parallel current destabilising peeling modes.

For the moment active control ELM tools are in the stage of the demonstration of the main principle followed by a study of the underlying physics. Further investigations will identify the applicability of these methods to Type I ELM control in ITER.

REFERENCES

[1]. M. Becoulet, et al., Contributions to Plasma Physics 40 (2000)251

[2]. M. Becoulet, et al., Plasma Phys Control Fus **44** (2002) A103

[3]. M. Becoulet, et al., Plasma Phys Control Fus 45 (2002) A93

[4]. K.H. Burrell et al Plasma Phys Control Fusion **44** (2002)A253

[5]. R.J. Buttery et al Nuclear Fusion **40**(2000)807

[6]. J.W. Connor, Plasma Phys Control Fus **40** (1998) 531

[7]. G.F. Consell et al Plasma Phys Control. Fusion, **44**(2002) 827

[8]. A.W. Degeling, et al., Plasma Phys Control Fusion **45** (2003) 1637

[9]. A.W. Degeling, YR Martin, JB Lister et al., Proc 2003 EPS Conf., ECA vol **27A** (2003) P-3.128

[10]. T. Eich et al Phys Rev Letters **91**(2003)N19

[11]. T. Eich et al J. Nucl. Mater. 313–316 (2003) 919

[12]. T.E. Evans Phys Rev Letters 2004 to be published

[13]. G. Federici et al Plasma Phys Control Fus **45** (2003) 1523

[14]. S.J. Fielding, RJ Buttery et al., Proc 2001 EPS Conf., ECA, **25A** (2001) 1825

[15]. T. Fujita Plasma Phys Control Fusion **44**(2002)A19

[16]. P. Ghendrih et al Plasma Phys. Control. Fusion, **38** (1996)1653

[17]. B.J. Green for the ITER Int. Team, Plasma Phys. Control. Fusion, **45** (2003)687

[18]. P. Gohil Plasma Phys. Control. Fusion **44** (2002)A37

[19]. L.D. Horton Nucl. Fusion **39**(1999)1

[20]. A. Hubbard et al Phys. of Plasmas, **8** (2001) 2033.

[21]. G.T.A. Huysmans et al Nucl. Fusion 38(1998)179

[22]. Yu. Igitkhanov et al "A Physics Picture of Type I ELMs" 28th EPS Conf. Control. Fusion and Plasma Physics, 2001, Contr. No P4.101

[23]. Y. Kamada et al. Plasma Phys. Control. Fusion **42** (2000) A247

[24]. Y. Kamada et al Plasma Phys. Control. Fusion **44** (2002)A279

[25]. K. Kamiya et al Nucl.Fusion **43** (2003)1214

[26]. K. Kamiya et al Plasma Phys. Control. Fusion **46** (2004)A157

[27]. K. Kamiya et al, submitted to Plasma Phys. Control. Fusion

[28]. P.T. Lang et al 28th EPS Conf. on Plasma Phys. and Contr. Fusion. Madeira, 25A(2001)P1.003

[29]. P.T. Lang et al., Nuclear Fusion **43** (2003) 1110

[30]. P.T. Lang et al., 30th EPS Conference on Contr. Fusion and Plasma Phys., St. Petersburg(2003) ECA Vol. 27A, P-1.129

[31]. L.L. Lao Plasma Phys. Control. Fusion **42** (2000) A51

[32]. A.W. Leonard et al. Plasma Phys Control Fusion **44** (2002) 945

[33]. A.W. Leonard, et al J Nuclear Mater 313-316,768(2003)

[34]. X. Litaudon et al Plasma Phys. Control. Fusion **46** (2004) A19

[35]. A. Loarte et al Comparison of high recycling H-modes on Alcator C-Mod and JET Bulletein of the Annual Meeting of the American Physics Soc.(Div.Plasma Physics), D01/4.

[36]. A. Loarte et al Plasma Phys Control Fus **44** (2002) 1815
[37]. A. Loarte et al., Plasma Phys Control Fus **45** (2003) 1549
[38]. A. Loarte et al Phys of Plasmas **11**(2004)2668
[39]. J. Lönnroth et al Plasma Phys Control Fus **46** (2004)767
[40]. J. Lönnroth et al Plasma Phys Control Fus **46** (2004)A249
[41]. S.C. McCool et al Nuclear Fusion **29**(1989)547
[42]. R.A. Moyer and T E Evans, 29th EPS Conf. on Plasma Phys. and Contr. Fus. Montreux, 26B(2002), P-1.063
[43]. D.A. Mossessian "H-mode edge stability of Alcator C-mod plasmas" Proc. 19th Int. conference (Lyon,2002) (Vienna: IAEA) EX/P5-04
[44]. I. Nunes et al, Proc 2003 EPS Conf., ECA vol **27A** (2003) P-1.157
[45]. N. Oyama et al, Nuclear Fusion **43** (2003) 1250
[46]. N. Oyama et al, Nuclear Fusion **44** (2004) 582
[47]. N. Oyama Private communication. To be published.
[48]. V.Parail V et al 28th EPS Conf. on Plasma Phys. and Contr. Fusion. Madeira, 25A(2001)P5.027
[49]. C.P. Perez et al., Plasma Phys Control Fusion **46** (2004) 61
[50]. A.R. Polevoi et al. Nuclear Fusion **43** (2003) 1072
[51]. J. Rapp et al Nucl.Fusion **44** (2004)312
[52]. A.B. Rechester and MN Rosenbluth Phys Rev Lett **40**(1978)38
[53]. S. Saarelma et al Nucl. Fusion **43** (2003)262
[54]. G. Saibene et al., Nuclear Fusion **39** (1999) 1133
[55]. G. Saibene et al., Plasma Phys Control Fus **44**(2002) 1769
[56]. Y. Sakamoto et al., Plasma Phys. Control. Fusion **46** (2004) A299
[57]. A. Samain et al Phys Fluids **B5**(1993)471
[58]. R. Sartori et al Plasma Phys Control Fusion 46(2004)723
[59]. Y. Sarazin et al Plasma Phys. Control. Fusion 44(2002)2445
[60]. P.b. Snyder et al "ELMs and constrains on the H-mode pedestal: a model based on peeling ballooning modes", Proc. 19th Int. conference (Lyon,2002) (Vienna: IAEA).
[61]. J. Stober et al Nuclear Fusion,**41**(2001)1123
[62]. W. Suttrop Plasma Phys. Control Fusion 42 (2000) A1
[63]. W. Suttrop et al Plasma Phys Control Fusion 45 (2003)1399
[64]. H.R. Wilson et al Phys Plasmas **9** (2002) 1277
[65]. H. Zohm Plasma Phys. Control. Fusion 38 (1996) 105.

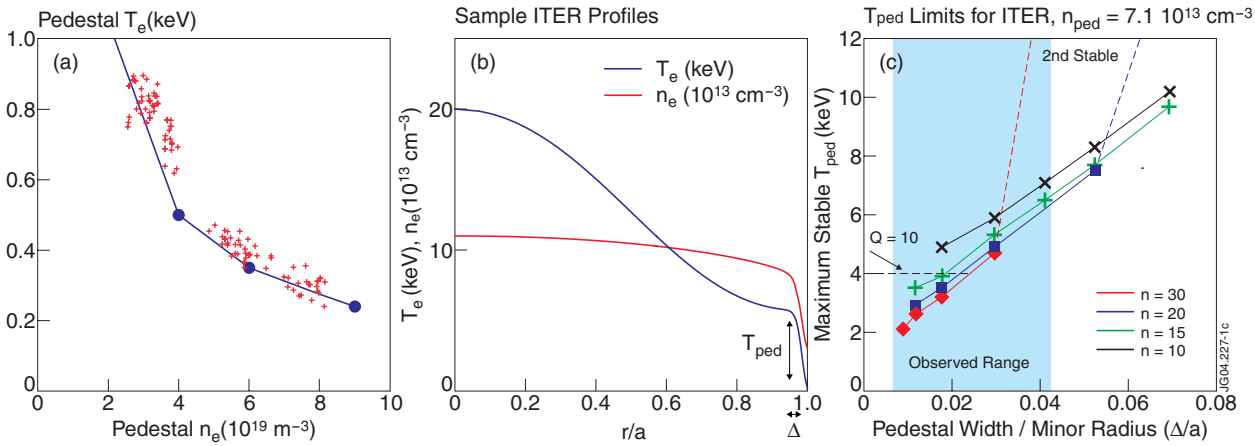

Figure 1:(a) Comparison of calculated pedestal stability boundaries to experimental data in DIIID. Calculated maximum temperature as a function of pedestal density (solid line) is compared to observed temperature and density before an ELM (crosses). (b) Typical electron temperature and density profiles foreseen for ITER H-mode scenario used in stability calculations. The pedestal width Δ is a parameter in modeling. At each value of Δ pedestal temperature is increased until the stability boundary is reached. The bootstrap current is calculated according to the profiles (c). The maximum stable pedestal temperature as a function of normalized pedestal width Δ for toroidal mode numbers n=10-30 in ITER. Plots from [60].

Figure 2: JETTO modelling results with the combined ballooning- peeling model for ELMs [40] (a) Typical ELM cycle in JETTO simulations. Points with equidistant separation in time (0.1ms) sampled at the magnetic surface ρ = 0.97. (b) Time trace of plasma current in ramp-up modelling by JETTO. (c) Perpendicular heat conductivity due to ELMs. (d)- ballooning modes growth rate in time . (e)- Peeling modes growth rate. (f)- Thermal energy content.

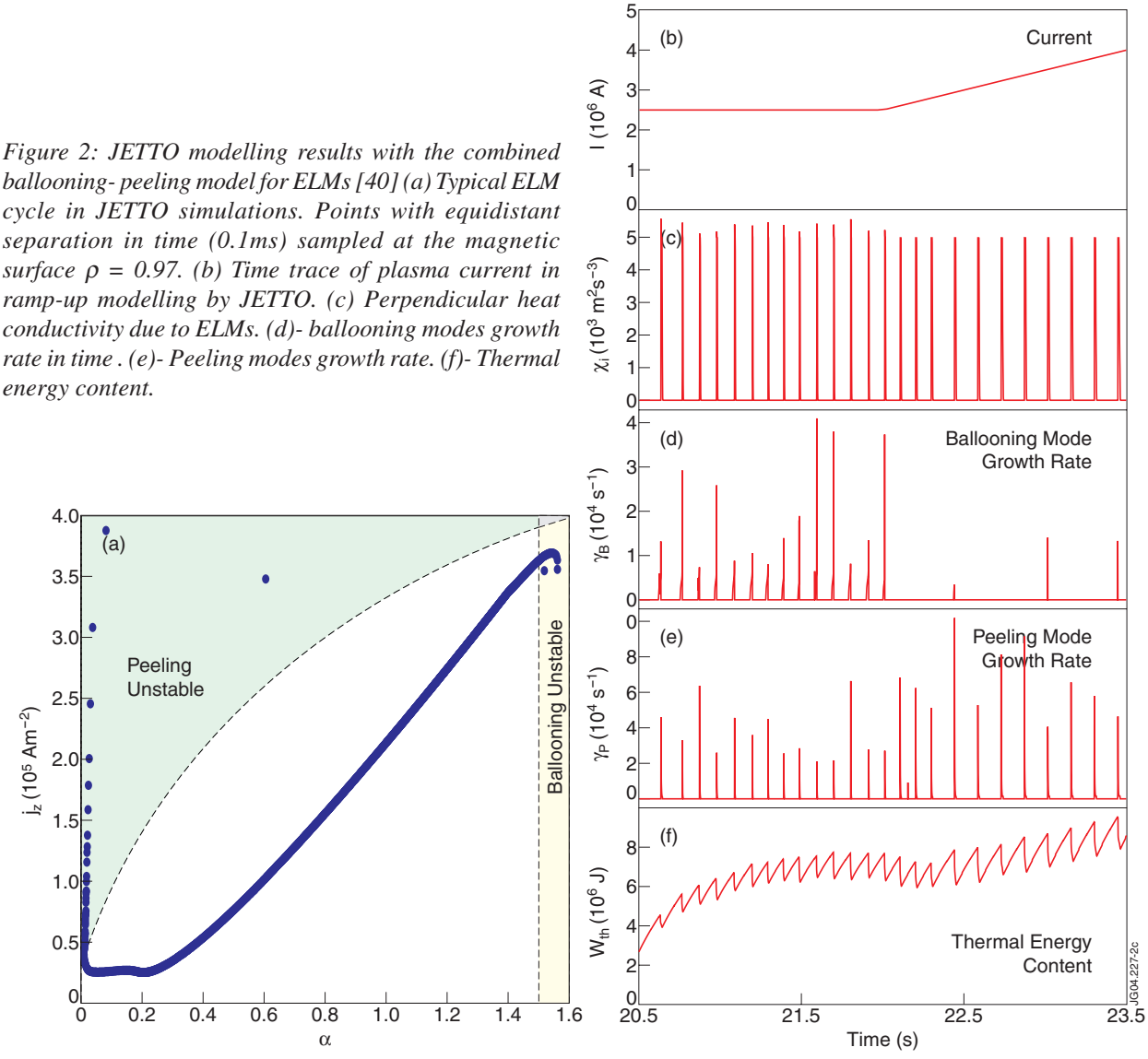

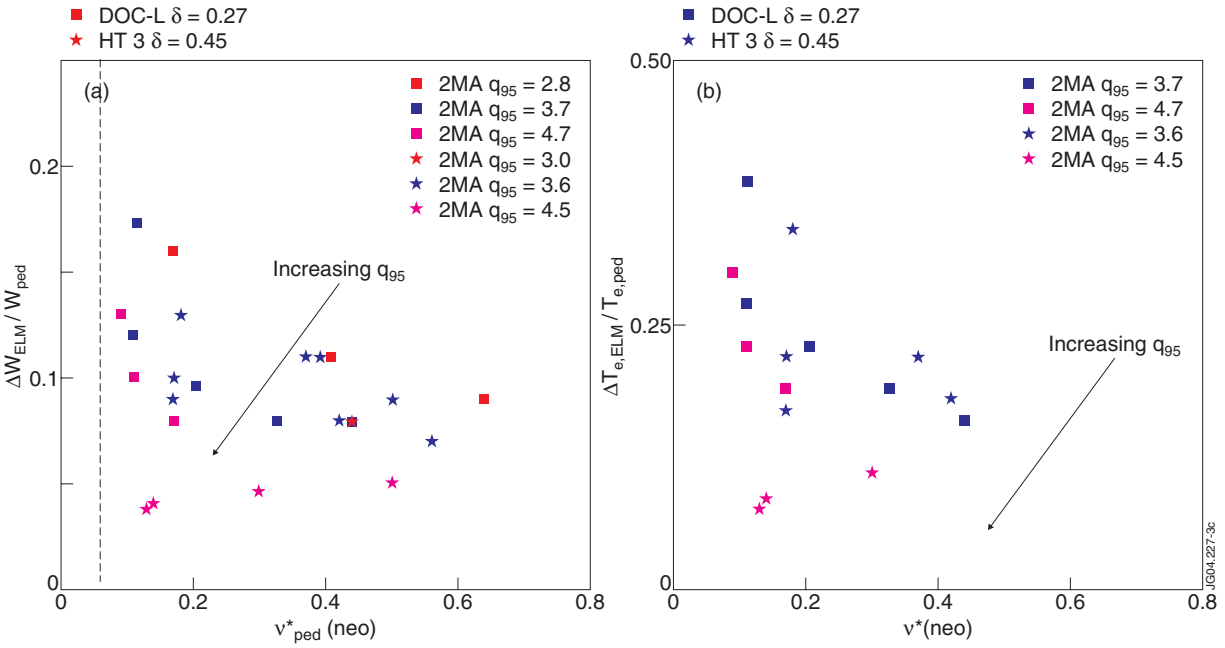

Figure 3: (a) Normalized ELM energy loss to the pedestal energy versus pedestal plasma collisionality for different q95 in JET for medium and high triangularity (δ). ELM energy loss is smaller for higher δ=0.45 and higher q95=4.5. (b) Normalized pedestal electron temperature drop in ELM versus pedestal plasma collisionality in the same scans. Figures from [38].

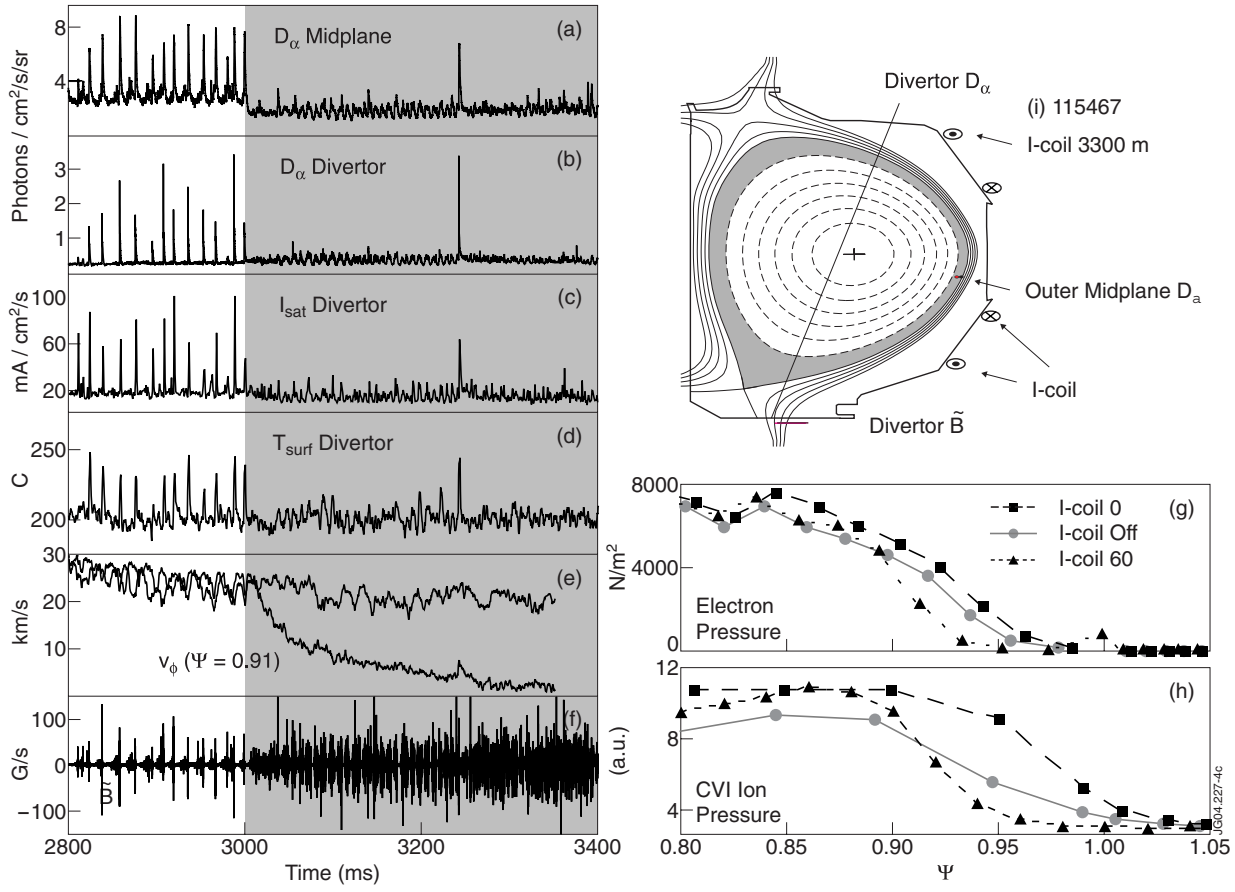

Fig.4. ELM suppression during discharge 115467 in DIII-D using stochastic boundary created by the I–coil perturbation. D_α recycling response from the midplane (a) and lower divertor (b) chords are shown with the particle flux to a Langmuir probe (c) and the surface temperature from an IR camera view (d) near the outer strike point in the lower divertor. The edge toroidal rotation (e) is shown with (black) and without (grey) the I–coil. Also shown is the lower divertor (f) magnetic fluctuation (Mirnov) signal. The shaded region indicates the time when the I–coil is pulsed on with a current of 4.4 kA. Electron pressure P_e (g)and CVI impurity pressure P^{CVI} profiles (h) with (black dashed) two discharges with I–coil pulses having 0° toroidal phase (filled squares) and 60° toroidal phase (filled triangles) are shown. (i)-EFIT equilibrium for the discharge 115467 in DIII-D and I-coils position . Figures from [12].

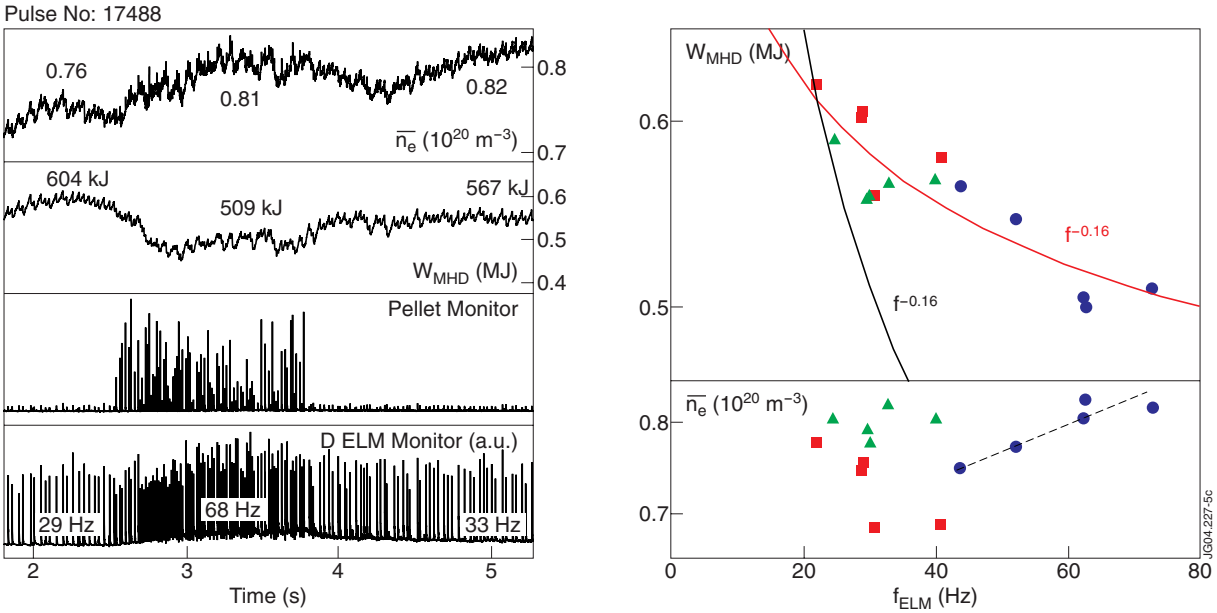

Figure 5: Left: Density, diamagnetic energy, pellet monitor and Da signals during external gas puff without pellets (f_{ELM}=29Hz), small pellets and no puff (f_{ELM}=68Hz) and with external puff only (f_{ELM}=68Hz). Right: Diamagnetic energy and line averaged electron density dependence on ELM frequency without gas (squares),gas puffed (triangles) and pellet phases (circles). Increasing f_{pel} imposes slight refuelling and confinement degradation. A fit to data with pellets:W_{MHD}~$f_{ELM}^{-0.16}$. Experimental scaling with gas puff in AUG W_{MHD}~$f_{ELM}^{-0.6}$. Figures from [30].

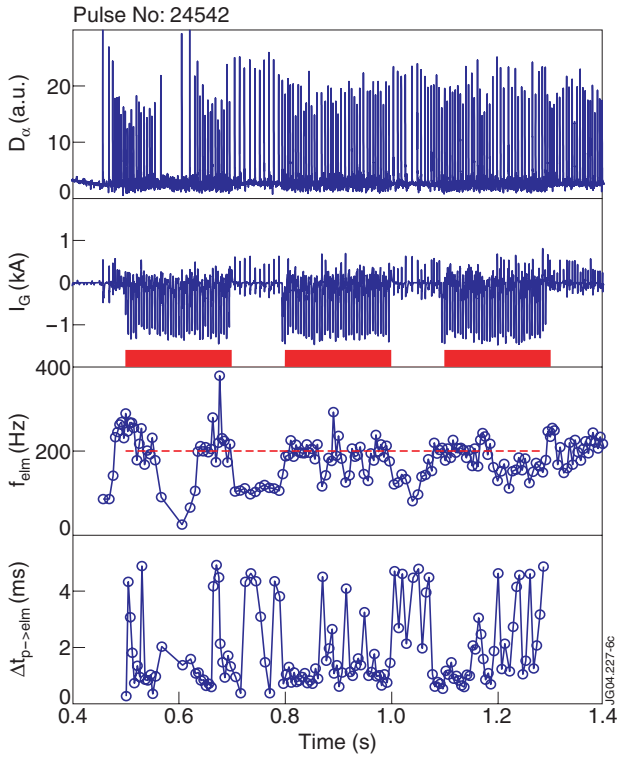

Figure 6: Example of Type III ELM frequency control by internal PF coils excitation in TCV Box 1: D_α signal, Box 2: PF coil current. Box 3: ELM frequency (dots) and frequency of the PF current perturbation (line), Box 4: Delay between each ELM and the previous current pulse in the coils. Figure from [9].